Surface critical exponents of self-avoiding walks on a square lattice with an adsorbing linear boundary: A computer simulation study

Hagai Meirovitch
Supercomputer Computations Research Institute, Florida State University, Tallahassee, Florida 32306-4052

Iksoo Chang
Research Center for Dielectric and Advanced Matter Physics and Department of Physics, College of Natural Sciences, Pusan National University, Pusan, Korea

(Received 1 March 1993)

Using the scanning simulation method, we study a model of a single self-avoiding walk (SAW) terminally attached to an adsorbing impenetrable linear boundary on a square lattice; an interaction energy ε ($\varepsilon<0$) is defined between the "surface" and a step (bond) that lies on the surface. SAW's of up to $N=260$ steps are studied from samples generated with different values of the scanning parameter, $b=3$ and 5. In most cases the different samples lead to the same results, which suggests that they are statistically reliable. At the ordinary point (infinite temperature T) our result for the growth parameter, $\mu=2.638\,16\pm0.000\,02$, is equal, within the error bars, to the best known estimate of Enting and Guttmann [J. Phys. A **18**, 1007 (1985)]. Also, our value $\gamma_1=0.9551\pm0.0003$ agrees very well with Cardy's value $\gamma_1=\frac{61}{64}=0.953\ldots$, obtained from conformal invariance [Nucl. Phys. B **240**, 514 (1984)]. At the special point, we obtain independently the estimates $\gamma_1=1.478\pm0.020$ and $\gamma_{11}=0.860\pm0.026$ and, therefore, also two independent estimates for μ that are found to be equal and very close to the Enting-Guttmann value. These results for γ_1 and γ_{11} satisfy the Barber scaling relation. However, our adsorption critical temperature $-\varepsilon/k_BT^*=K^*=0.722\pm0.004$ is larger than estimates previously obtained by the transfer-matrix method. Correspondingly, our result for the crossover exponent $\phi=0.562\pm0.020$ is significantly larger than a theoretical value of Burkhardt, Eisenriegler, and Guim [Nucl. Phys. B **316**, 559 (1989)], $\phi=\frac{1}{2}$.

PACS number(s): 36.20.Ey, 02.70.−c, 05.70.Jk, 64.60.Kw

I. INTRODUCTION

In recent years, a great deal of analytical results have been derived for polymers in two dimensions, mainly due to the advent of Coulomb-gas techniques and conformal invariance [1–7]. In particular, two fundamental phenomena have been studied extensively, the collapse of polymers at the Flory θ point and adsorption of polymers on a surface [8–10]. These phenomena have a wide range of industrial applications [11] and biological significance (e.g., protein folding [12]) and, therefore, understanding them, even in two dimensions, is important. It is also of interest to verify the predictions of the above-mentioned theories by studying realistic models of polymers using numerical techniques, such as exact enumeration [13–19], transfer matrix [20–25], or Monte Carlo [26–43]. Obviously, such techniques have their own drawbacks, the most severe being the fact that they are restricted to handling relatively small systems; however, in many cases numerical methods have been found to be useful in corroborating as well as in ruling out theoretical predictions.

In this paper we study a simple two-dimensional model of a single self-avoiding walk (SAW), terminally attached to an adsorbing impenetrable linear boundary; this model has recently regained interest in view of new theoretical results. Cardy [5] using conformal-invariance considerations, has derived the free-energy exponent $\gamma_1=\frac{61}{64}$ at high temperature, where the surface attractions are not effective (the magnetic ordinary point [10,33]). Also, Burkhardt, Eisenriegler, and Guim [6], employing similar techniques, have calculated the crossover exponent $\phi=\frac{1}{2}$ at the adsorption transition (the magnetic special point). The Cardy value has been corroborated by all numerical studies [13,14,19,24,25]; the $\phi=\frac{1}{2}$ result is supported by recent transfer-matrix [24,25], exact-enumeration [19], and Monte Carlo [38] calculations, while previous studies have been found to be inconclusive [16,44,45].

However, all these investigations are based on relatively small systems and it is therefore of interest to check the behavior of longer chains; this is achieved here by applying the scanning simulation method, which has been found suitable to handle models of polymers near a surface [34,37,41]. With this method a chain is generated step by step with the help of transition probabilities, which are obtained by scanning all the possible chain continuations in b future steps; the larger b is, the better the probabilities and the longer the chains that can be simulated efficiently. We carry out extensive simulations of relatively long chains of up to 260 steps in the two regimes and calculate the transition temperature ϕ, the values of γ_1, and, independently, those of the exponent γ_{11}. The same results are obtained from samples generated with $b=3$ and 5, which constitutes an important test

that these results are statistically reliable. While at the ordinary point our result for γ_1 agrees with the Cardy value, our result for ϕ is significantly higher than the theoretical value, $\phi=\frac{1}{2}$.

II. THE MODEL AND THERMODYNAMIC FUNCTIONS

The model studied is a single self-avoiding walk of N steps (bonds) (i.e., $N+1$ monomers) which starts from the origin located on an adsorbing impenetrable linear boundary on a square lattice. Attractive interaction ε ($\varepsilon<0$) is defined between a bond that lies on the surface and the surface (this definition differs from the traditional one in which a monomer at the surface, rather than a bond, gains energy [46]); the microscopic surface energy is $E_i=\varepsilon m_i$, where m_i is the number of bonds on the surface for SAW configuration i. Thus, two partition functions Z_α are defined

$$Z_\alpha=\sum_i{}^{\alpha}\exp(-E_i/k_BT) , \tag{1}$$

where k_B is the Boltzmann constant and T is the absolute temperature; $\alpha=1$ denotes the usual partition function, while $\alpha=11$ means that the summation is carried out only over the subgroup of SAW's which also end on the surface. The Boltzmann probability of i is

$$P_i^B=\exp(-E_i/k_BT)/Z_1 . \tag{2}$$

Thus, the average surface energy E per ε reads

$$E=\varepsilon^{-1}\sum_i P_i^B E_i . \tag{3}$$

It proves convenient to define the surface reciprocal temperature $K=-\varepsilon/k_BT$, where the corresponding critical value is denoted by K^*. The partition functions defined above [Eq. (1)] lead to the free energies

$$F_\alpha=\sum_i{}^{\alpha}P_i^B(E_i+k_BT\ln P_i^B) . \tag{4}$$

III. THE SCANNING METHOD

With the scanning method [40], a chain is generated step by step with the help of transition probabilities which are obtained by scanning b future steps. At step k of the process, $k-1$ directions (steps) of the chain have already been constructed and one seeks to determine the kth direction ν_k, where ν can have four values on a square lattice. For that, one uses the notion of a future SAW [40], which is a possible continuation of the partial SAW (of $k-1$ steps) in b future steps; b is called the scanning parameter. One then defines a future partition function $Z_k(\nu,b)$,

$$Z_k(\nu,b)=\sum_j\exp(-\varepsilon m_j/k_BT) , \tag{5}$$

where j runs over all the future SAW's of b steps that start at direction ν and m_j is the number of bonds (steps) of j that lie on the surface. The transition probability for direction ν, $p_k(\nu,b,f)$ is

$$p_k(\nu,b,f)=Z_k(\nu,b)f^{\nu\cdot u}\Big/\sum_\nu Z_k(\nu,b)f^{\nu\cdot u} , \tag{6}$$

where f is a mean-field parameter $\mathbf{u}$ is a unit vector in the $+y$ direction, and $\boldsymbol{\nu}$ is a unit vector which points in the direction ν ($\nu=1,4$). f has been introduced [34] in order to compensate for the fact that for a remote monomer ($y>b$) the future chains cannot "sense" the surface. Thus, at $T>T^*$, the effect of the surface is to repel the chain in the $+$y direction; therefore, one would expect $f>1$, while for low enough T ($T<T^*$), $f<1$. Notice that for a direction which is parallel to the surface, $f^{\nu\cdot\mathbf{u}}=1$. Thus, ν_k is selected with the help of a random number and the process continues. Once the N-step chain i has been generated, one knows its construction probability $P_i(b,f)$:

$$P_i(b,f)=\prod_{k=1}^{N}p_k(\nu_k,b,f) , \tag{7}$$

which is the product of the N sequential transition probabilities with which the directions $\nu_1,\ldots,\nu_N$ have been chosen. For a practical value of b the future can be scanned only partially; therefore, the SAW may get to a dead end during construction. In this case the (partial) chain is discarded and a new one is started. The efficiency of the process to generate SAW's can be expressed by the attrition ratios

$$A_\alpha=n_\alpha/n_0 , \tag{8}$$

where n_0 is the number of chains attempted, n_1 is the number of chains succeeded, and n_{11} is the number of successful chains that also end on the surface. Obviously, A_{11} is considerably smaller than A_1.

The occurrence of failures also means that $P_i(b,f)$ [Eq. (7)] (in contrast to P_i^B [Eq. (2)]) is not normalized over the ensemble of SAW's, but over a larger ensemble which also consists of self-intersecting walks, i.e.,

$$\sum_{\text{SAW's}}P_i(b,f)=G<1 . \tag{9}$$

A normalized probability $P_i'(b,f)$ can be defined by

$$P_i'(b,f)=P_i(b,f)/G , \tag{10}$$

where $P_i'(b,f)$ is approximate (biased) (for more details, see Refs. [34] and [40]).

Using the biased $P_i'(b,f)$ [Eq. (10)], one can define the approximate free-energy functional $F_1(b,f)$:

$$F_1(b,f)=\sum_{\text{SAW's}}P_i'(b,f)[E_i+k_BT\ln P_i'(b,f)] , \tag{11}$$

which is expected to overestimate the correct free energy F_1 [Eq. (4)]. This enables one to determine the optimal value of the mean-field parameter f by minimizing $F_1(b,f)$ with respect to f for a given value of b, which is achieved by carrying out several relatively short simulations with different values of f.

Since $F_1(b,f)$ is biased, one uses importance sampling to obtain unbiased *estimations*, $\bar{F}_\alpha$ (IS) of the exact free energies F_α [Eq. (4) [27,47,48]:

$$\bar{F}_\alpha(\mathrm{IS}) = -k_B T \ln \left[n_0^{-1} \sum_{t=1}^{n_\alpha} \exp\left[-\frac{E_{i(t)}}{k_B T} \right] \Big/ P_{i(t)}(b,f) \right] , \tag{12}$$

where $i(t)$ is the tth SAW generated with the scanning procedure and n_α and n_0 are defined in Eq. (8). A similar estimation, $\bar{E}(\mathrm{IS})$, can also be defined for the average energy E [Eq. (3)]. Another way to remove the bias is by a procedure due to Schmidt [40,49] in which an effectively smaller sample (the accepted Boltzmann sample) is extracted from the biased one. Thus, n_{accept}, the number of *different* chains accepted to the unbiased sample, serves as the effective sample size for the importance sampling results. A useful parameter of efficiency is the acceptance rate

$$R_I = n_{\mathrm{accept}}/n_0 , \tag{13}$$

which is expected to increase as the bias is decreased, becoming 1 for an unbiased (Boltzmann) sample. Thus, the optimal value of the mean-field parameter can also be determined by maximizing R_I with respect to f. In practice, R_I is expected to decrease exponentially with increasing N.

An important check for the reliability of the importance-sampling procedure is to carry out simulations with different values of b, verifying that the results for $\bar{F}_\alpha(\mathrm{IS})$ and $\bar{E}(\mathrm{IS})$ are not changed as b is increased. Thus, we have performed at least two simulations at each temperature using $b=3$ and 5. However, it should be emphasized that this check does not always provide a complete guarantee for statistical reliability. In principle, there might be configurations that, while making a significant contribution to the averages, are very improbable with the value of b studied and therefore would not be represented even in a large sample (see the discussion in Ref. [40]).

IV. RESULTS AND DISCUSSION

A. Efficiency of the scanning method

Using the scanning method, we generated samples of SAW's of length $N=260$. In order to investigate the dependence of various properties on N, their importance-sampling values [Eq. (12)] were calculated and accumulated for the partial chains of lengths 10,20, . . . , 260. As in previous studies, the search for the transition temperature K^* is based on the fact that with importance sampling [Eq. (12)], results at *many* different temperatures can be obtained from a *single* sample simulated at a given temperature [33,34,37,39,41]. Thus, in order to determine K^*, we have generated three samples, two with a scanning parameter $b=3$, at $K=0.730$ [$n_0=50\times10^6$; see Eq. (8)] and at $K=0.718$ ($n_0=95\times10^6$), and one with $b=5$ at $K=0.718$ ($n=123\times10^6$). For each simulation, results were also calculated at the 20 temperatures,

$$K=0.700, 0.702, \ldots, 0.738 .$$

In order to study the ordinary point, two samples were generated at infinite temperature ($K=0$), with $b=3$ ($n_0=50\times10^6$) and $b=5$ ($n_0=128\times10^6$). For all these samples we have used a mean-field parameter f [Eq. (6)] which is larger than 1, $f=1.1$ for the K^* samples, and $f=1.2$ for the $K=0$ ones, which means that f is more effective for $K=0$ than for K^*. Also, we have found that the simulations become more efficient (i.e., the results for $F_1(b,f)$ [Eq. (11)] are smaller and those for the acceptance rate R_I [Eq. (13)] are higher) if for $y \le b$ we use $f=1$; in other words, when the future chains can "feel" the surface, it is preferable to "switch off" the effect of f.

A sample of $n_0=5\times10^6$ requires $\sim$85 h of CPU time on the IBM340 RISC 6000 computer workstation using $b=5$ and approximately half of this time for $b=3$. In Table I results are presented which demonstrate the

TABLE I. Results that demonstrate the efficiency of the scanning method. They were obtained at the critical temperature $K^*=0.722$ and at $K=0$ for various values of chain length N. A_1 [Eq. (8)] is the attrition ratio; A_{11} [Eq. (8)] is the attribution ratio for SAW's that also end on the surface. R_I [Eq. (13)] is the acceptance rate and n_{accept} is the number of accepted SAW's. F_1 (IS) [Eq. (12)] and $\bar{E}$(IS) are the importance sampling estimates of the free energy and the energy [Eq. (3)], respectively. The results for $\bar{F}_1$(IS) and $\bar{E}$(IS) were obtained from partial samples. The statistical error is one standard deviation [2.45(1)=2.45±0.01].

N	A_1	A_{11}	R_I	$10^{-3}\, n_{\mathrm{accept}}$	$\bar{F}_1(\mathrm{IS})Nk_BT$	$\bar{E}(\mathrm{IS})/N$
			$K=0.722$			
80	0.85	0.028	0.42	51,406	−1.000 28(1)	−0.1463(2)
140	0.68	0.012	0.20	24,787	−0.989 39(2)	−0.1143(3)
200	0.53	0.0064	0.10	12,182	−0.984 56(3)	−0.098(1)
250	0.43	0.0039	0.055	6,602	−0.982 15(1)	−0.089(2)
			$K=0$			
80	0.88	0.012	0.40	51,297	−0.968 95(1)	
140	0.74	0.0051	0.22	27,760	−0.969 26(1)	
200	0.61	0.0024	0.12	15,141	−0.969 42(2)	
250	0.52	0.0013	0.072	9,191	−0.969 52(2)	

efficiency of the scanning method; they were obtained from the samples generated with $b=5$ at $K=0$ and at $K^*=0.722$, which is the central value of the transition temperature found in this work. As expected, the results for the attrition ratios A_1 and A_{11} [Eq. (8)], the acceptance rate R_I [Eq. (13)], and n_{accept} decrease strongly with increasing chain length N, where the efficiency at $K=0$ is slightly better than at $K^*=0.722$ (the values of R_I of the latter are the smaller). On the other hand, as one would expect, the results for the attrition ratios A_{11} are lower (by a factor of 2 to 3) at infinite temperature than at $K=0.722$ due to the large entropic repulsion exerted on the chain by the surface at a high temperature. Therefore, much larger samples are required for estimating γ_{11} $(K=0)$ than $\gamma_{11}(K^*)$; indeed, the relatively large sample generated at $K=0$ stems from that reason. A limited check of the reliability of the results can be achieved by comparing them, for $N=10$ and 20, to the exact-enumeration values [16]. The agreement is indeed excellent. From $N=20$ and $K=0.722$, we obtain $\bar{E}(\text{IS})/N=0.267\,36$, as compared to the exact value, 0.267 40, and

$$F(\text{IS})/Nk_BT=-1.057\,184 \text{ versus } -1.057\,188 .$$

B. The special point

The surface critical temperature K^* was determined from the expected behavior of the energy E [Eq. (3)] at K^*, the transition temperature [33],

$$E\sim N^{\phi} , \tag{14}$$

where ϕ is a crossover exponent smaller than 1; at the cold region, $K>K^*$, the energy of a very long chain becomes extensive ($\sim N$), while in the hot region, E is constant, i.e., it does not increase with increasing N. Therefore, a log-log plot of the results for E/N versus N for different values of K would lead to a straight line at K^* with a negative slope, $\phi-1$. The slope of a line in the hot region is expected to decrease as N increases, becoming -1 for a very long chain. In the cold region, on the other hand, the slope will increase towards 0 as N increases. In Fig. 1 results for E/N versus N are shown in a log-log plot for different temperatures and the three different regimes are clearly demonstrated, where an approximately straight line occurs at $K=0.722$.

However, K^* can also be determined using a more accurate procedure [50]; at K^* one expects (if corrections to scaling are ignored), $E(2N)/E(N)=2^{\phi}$, which is a constant. These ratios for $N=10,20,\ldots$ (for simplicity we shall omit the values of $2N$) can be plotted as a function of K, where the intersection point of the lines (at which the above energy ratios become constant) defines both K^* and ϕ. In Fig. 2 such a plot is presented for the $b=5$ sample, where the results for $N=10$, 20, and 30 are omitted due to strong correction to scaling effects; we have also omitted the results for the longest chains, $N=110$ and 120, which are less statistically reliable. The figure reveals that the lines intersect at $K=0.722$. However, determination of K^* requires a carefully balanced analysis in which a larger weight is given to the data of the longer chains while verifying their statistical reliability. We have found that the lines based on $N=10$ and 20 intersect at $K>0.738$, while those based on $N=20$ and 30 and $N=30$ and 40 intersect at the monotonically decreasing values, $K=0.732$ and 0.726, respectively. However, the intersections of the lines based on $N=40$ and 50, 50 and 60, and 60 and 70 all occur at $K=0.722$ (i.e., they cover the range $40\le N\le 140$; notice again that the values $2N$ are omitted). These results have also been obtained for the two samples generated with $b=3$, which constitutes a credible check that the importance-sampling results are reliable and that they are not affected by the different temperatures at which the simu-

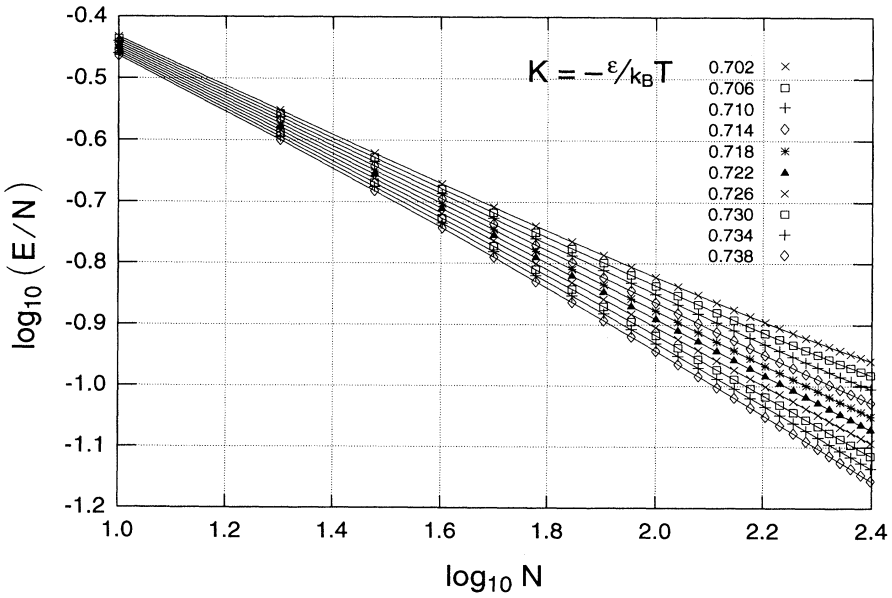

FIG. 1. Log-log plots of the average energy per step, E/N [Eqs. (3) and (14)] vs chain length N for different reciprocal temperatures $K=0.702$, $0.706,\ldots,0.738$. An approximately straight line is observed at $K=0.722$ (solid triangles), which is identified with the critical temperature K^*.

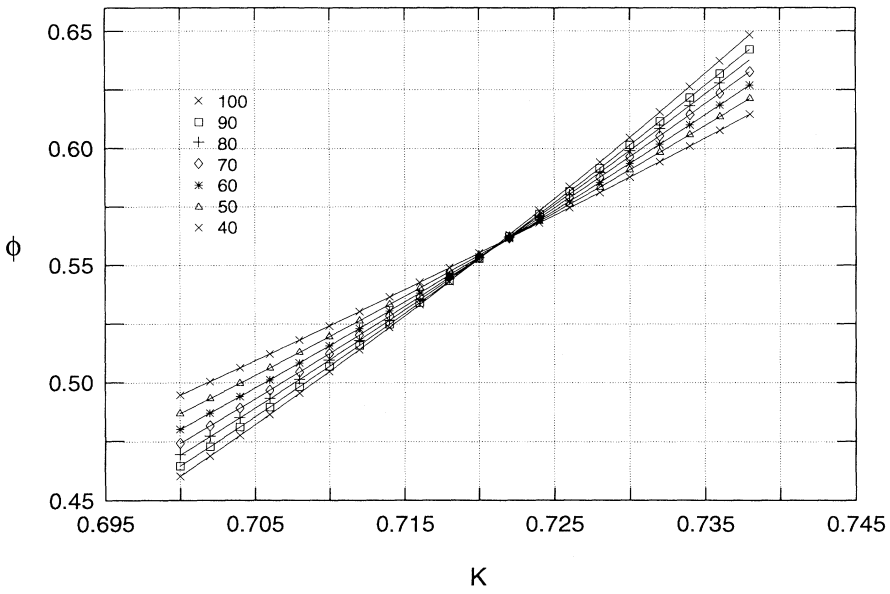

FIG. 2. Plots of the energy ratios $\log_{10}[E(2N)/E(N)]/\log_{10}2$ vs the temperature K for $N=40,50,\ldots,100$. The intersection point (at $K=0.722$) defines both the critical value K^* and the crossover exponent ϕ.

lations were performed.

For the longer chains, i.e., $N=70$ and 80, 80 and 90, and 90 and 100, the intersections depend on the sample. Thus, for the samples generated with $b=3$, the data were found to be statistically unreliable (the lines in a graph similar to that presented in Fig. 1 were "bumpy"). For the $b=5$ partial sample (of $n_0=73\times10^6$), the corresponding intersections occurred at $K=0.720$, 0.720, and 0.718, while increasing this sample to $n_0=123\times10^6$ increased these values to $K=0.720$, 0.722, and 0.720, respectively. Therefore, we expect that increasing the sample size further would increase all these values to 0.722. The intersections for $N>100$ have been found to occur at $K=0.714$; however, such a relatively large decrease in the value of K is not expected to occur within the small range $N=200$–240 and, therefore, these results are considered to be statistically unreliable (see the relatively low values of n_{accept} for $N=200$ and 250 in Table I). Thus, it is difficult to decide on the basis of these results whether the monotonic decrease of the values of K^* observed for the shorter chains would continue beyond $K=0.722$ for longer chains. Our estimates for K^* and ϕ are

$$K^*=0.722\pm0.004,\quad \phi=0.562\pm0.020\ ,$$

where the errors here and in the rest of the paper are 95% confidence limits. The central value of ϕ is that obtained at $K^*=0.722$ ($N=40$–100), while the error $\pm D$ is based on the maximal deviation from the central value of the results for ϕ at $K=0.726$ and 0.718. Thus,

$$D(0.718)=0.652-\phi(0.718)+D'\ ,$$

where $\phi(0.718)$ is the average value of the results for ϕ at $K=0.718$ based on $N=40$–100 (the results do not meet at a point); D' is the maximal deviation from the average value and

$$D=\max[D(0.718),D(0.726)]\ .$$

Our results for K^* are slightly larger than those obtained by other methods which are based on extrapolation of exact results for relatively small systems. Ishinabe [16] has obtained $K^*=0.718$ and 0.698 from two different analyses of exact-enumeration data for SAW's of $N\le21$ (no error bars have been provided), while Kremer [45] obtained from real-space renormalization, $K^*=0.65\pm0.05$. More recent transfer-matrix studies of Guim and Burkhardt [24] and Veal, Yeomans, and Jug [25] have led to $K^*=0.713\pm0.002$ and 0.714 ± 0.003, respectively. A similar result, $K^*=0.715\pm0.001$, was also obtained by Foster, Orlandini, and Tesi [19] who exact-enumerated longer chains than Ishinabe, of $N\le28$.

Our result for ϕ is significantly larger than the theoretical value of Burkhardt, Eisenriegler, and Guim [6], $\phi=\frac{1}{2}$, obtained from conformal-invariance considerations (see also Ref. [4]); notice that $\frac{1}{2}$ has been found by Bouchaud and Vannimenus [51] to constitute an upper-bound value for ϕ. Previous numerical studies are not accurate enough to shed light on this discrepancy. The Ishinabe values are 0.50 and 0.53, whereas Kremer estimated $\phi=0.55\pm0.1$ from the Ishinabe data and obtained 0.55 ± 0.15 from real-space renormalization; a Monte Carlo study [38] of relatively short chains ($N\le100$) and small samples, based on a variant of the Rosenbluth [27] procedure (i.e., $b=1$), has led to $\phi=0.51$. On the other hand, the values obtained in the transfer-matrix studies agree with $\phi=\frac{1}{2}$; the value of Ref. [24] is 0.501 ± 0.003, while from Ref. [25] we have calculated two estimates, $\phi=0.51\pm0.01$ and 0.521 ± 0.001. Also, recent transfer-matrix calculations for strips with one and two ordering edges by Guim and Burkhardt [52] are again consistent with $\phi=\frac{1}{2}$. The reason for the disagreement between our and the transfer-matrix results is not clear. As far as our simulation is concerned, there is still a possibility that the correct value of K^* is smaller than 0.722 and it would be obtained only for very long chains; this would also cause

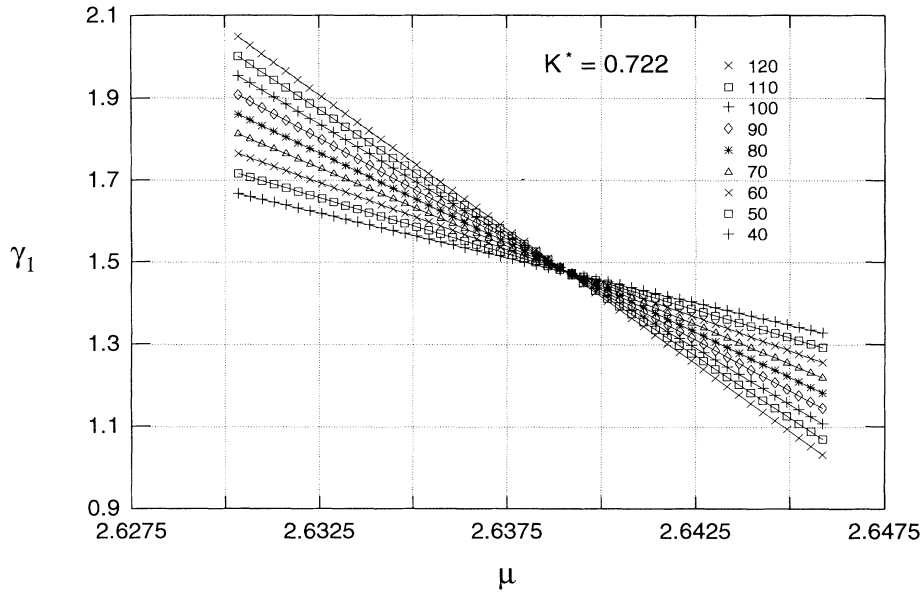

FIG. 3. Plots of the free-energy ratios $\log_{10}[2(Z_1(2N)/Z_1(N)\mu^N]/\log_{10}2$ vs the growth parameter μ for $N=40, 50, \ldots, 120$ at the critical temperature $K^*=0.722$ [Eqs. (1), (4), and (12)]. The intersection point defines both the correct μ and the exponent $\gamma_1(K^*)$.

a decrease in the value of ϕ. However, notice that according to Fig. 2, $\phi=\frac{1}{2}$ corresponds approximately to $K=0.706$ and such a significant change in the value of K^* is very unlikely [see the results for $K^*(N)$ in Ref. [34]].

The partition functions Z_α [Eq. (1)] can be obtained by importance sampling [Eqs. (4) and (12)]; at K^* their expected behavior is

$$Z_\alpha = B_\alpha \mu^N N^{\gamma_\alpha - 1} , \tag{15}$$

where B_α is a prefactor and μ, the growth parameter, has the same value as for SAW's in the bulk. In order to calculate μ and γ_α, we used the same method described above for specifying K^* and ϕ. Thus, at K^*, Eq. (15) leads to

$$2Z_\alpha(2N)/Z_\alpha(N)\mu^N = 2^{\gamma_\alpha} , \tag{16}$$

and one can calculate for each pair $(N,2N)$ the values of $2Z_\alpha(2N)/Z_\alpha(N)\mu^N$ for different values of μ, where the intersection point of these lines should define the correct values of both γ_α and μ. In Fig. 3 such a plot is presented at $K^*=0.722$ for γ_1 for $N=40,50,\ldots,120$, and a sharp intersection point is observed. In Table II are given the intersection values of γ_1 and μ obtained for similar graphs based on different number of lines. For each quantity these results fluctuate only slightly and the average values were taken as our best central estimates:

$$\gamma_1(K^*)=1.478\pm0.020, \quad \mu=2.6391\pm0.0006 .$$

The error bars have been obtained in the same way as for ϕ, i.e., by calculating tables like Table II at $K=0.718$ and 0.726 and determining the maximal deviations from the above central values.

A graph similar to that of Fig. 3 but based on the re-

TABLE II. Intersection values for the growth parameter μ and the exponent γ_1 at $K^*=0.722$. These results were obtained from figures similar to Fig. 3 for different numbers of intersecting lines $(N,2N)$; for example, the results for $N=40$–120 are based on the intersection of the lines defined by (40,80),(50,100), . . . ,(120,240). Our central values of γ_1 and μ are obtained by averaging the values in the table (for details, see the text).

N \ N	120	110	100	90	80	70
			γ_1			
40	1.476	1.476	1.476	1.473	1.473	1.473
50	1.481	1.476	1.476	1.477	1.477	
60	1.481	1.481	1.481	1.477		
70	1.481	1.481	1.481			
			μ			
40	2.6391	2.6391	2.6391	2.6392	2.6392	2.6392
50	2.6390	2.6391	2.6391	2.6391	2.6391	
60	2.6390	2.6390	2.6390	2.6391		
70	2.6390	2.6390	2.6390			

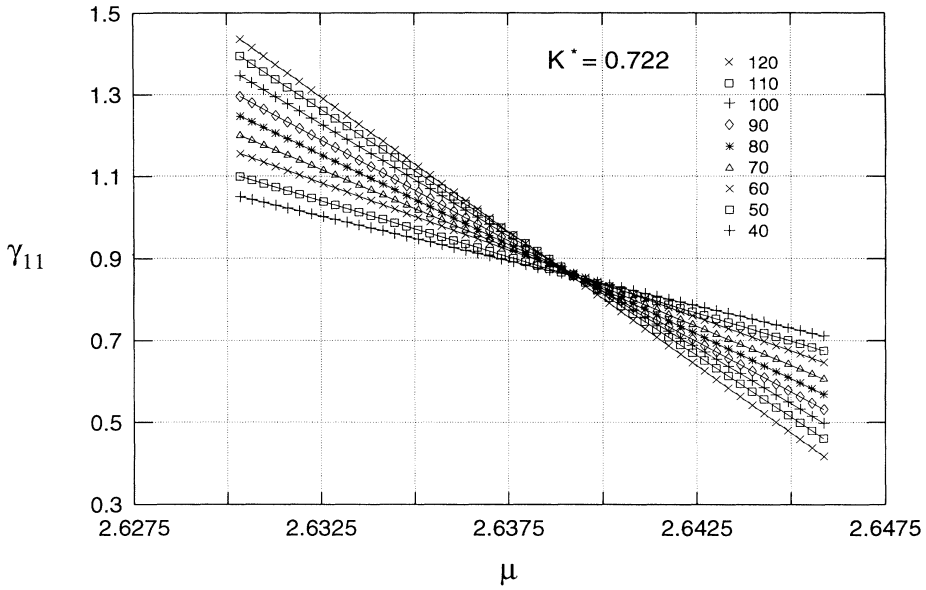

FIG. 4. Plots of the free-energy ratios for SAW's that also end on the surface [Eqs. (1), (4), and (12)], $\log_{10}[2(Z_{11}(2N)/Z_{11}(N)\mu^N]/\log_{10}2$ vs μ for $N=40,50,\ldots,120$ at the critical temperature $K^*=0.722$. The intersection point defines both the correct μ and the exponent $\gamma_{11}(K^*)$.

sults of $\bar{F}_{11}$(IS) [Eq. (12)] is presented in Fig. 4 for $N=40-120$. Again, a sharp intersection point is observed which defines the values of μ and γ_{11}. In order to obtain the central values and the error bars for these quantities, we have carried out the same analysis as described above for γ_1, i.e., averaging the corresponding results in Table III and calculating their deviations from results obtained at $K=0.718$ and 0.726; the results are

$$\gamma_{11}(K^*)=0.860\pm0.026, \quad \mu=2.6392\pm0.0009 .$$

It should be noted first that, unlike in previous simulation studies of adsorption of chains to a surface [33,34,37,41], the values of μ obtained here from the two partition functions are equal. This is probably due to the relatively large sample generated, which enables us to obtain a good estimation of Z_{11}. For $K\leq K^*$, the value of μ is expected to be equal to that of SAW's in the bulk. However, the above results are slightly larger, even with the error bars, than the value 2.638 159(1) obtained by Enting and Guttmann [53] for self-avoiding rings in the bulk. This indicates that our results are not free from finite-size effects and longer chains should be studied. The best value of μ, $\mu=2.6429$, obtained by Guim and Burkhardt [24] from a transfer-matrix analysis (without extrapolation, however), is also too large, while Veal, Yeomans, and Jug [25] provide two extrapolations, 2.6380(2) and 2.639(2), both equal to the Enting and Guttmann value, within the error bars.

Our central value of γ_1 is larger than the theoretical value of Guim and Burkhardt [24], $\gamma_1=\frac{93}{64}=1.453\ldots$ as well as their numerical estimate, $\gamma=1.454(4)$; by Veal, Yeomans, and Jug [25], 1.4502(1); and by Foster, Orlanding, and Tesi [19], 1.460(4); however, for the latter estimate, the errors overlap. Notice that, in contrast to the present work, these studies do not provide an independent estimation of γ_{11}. Our values of γ_1 and γ_{11} satisfy very nicely the Barber [54,13] surface scaling relation $2\gamma_1-\gamma_{11}=\gamma+\nu$; the exact bulk values lead to $\frac{43}{32}+\frac{3}{4}=\frac{67}{32}\sim2.094$, while our results yield

$$2\gamma_1-\gamma_{11}=2.096\pm0.066 .$$

TABLE III. Same as Table II for μ and the exponent γ_{11} at $K^*=0.722$, based on figures similar to Fig. 4.

N \ N	120	110	100	90	80	70
			γ_{11}			
40	0.864	0.856	0.856	0.856	0.856	0.850
50	0.865	0.856	0.856	0.856	0.857	
60	0.870	0.866	0.866	0.874		
70	0.870	0.855	0.855			
			μ			
40	2.6391	2.6393	2.6393	2.6393	2.6393	2.6495
50	2.6391	2.6393	2.6393	2.6393	2.6393	
60	2.6390	2.6391	2.6391	2.6389		
70	2.6390	2.6393	2.6393			

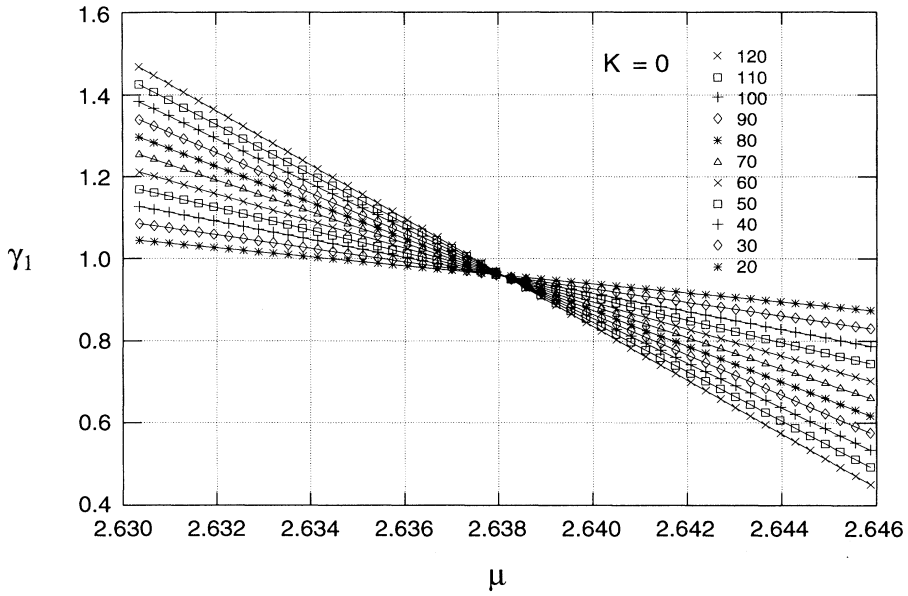

FIG. 5. Plots of $\log_{10}[2Z_1(2N)/Z_1(N)\mu^N]/\log_{10}2$ vs μ for $N=20,30,\ldots,120$ at infinite temperature $K=0$ (see Fig. 3 caption). The intersection point defines both the correct μ and γ_1 $(K=0)$.

C. The ordinary point

In order to investigate the ordinary transition, we have simulated the same model at infinite temperature, i.e., at $K=0$. Two samples of $n_0=70\times10^6$ and 128×10^6 attempted chains were generated using scanning parameters $b=3$ and 5, respectively. Graphs similar to those of Figs. 3 and 4 are presented in Figs. 5 and 6 for γ_1 and γ_{11}, respectively. Figure 4 demonstrates a sharp intersection point that consists of $N=20-120$, which means that corrections to scaling are small. In Table IV results are shown for γ_1 and μ obtained (as in Table II) for different numbers of intersecting lines. Our central values for γ_1 and μ are obtained by averaging these results, where the statistical errors are twice the corresponding standard deviations:

$$\gamma_1(K=0)=0.9551\pm0.003\ ,$$

$$\mu=2.638\,16\pm0.000\,02\ .$$

The above value of μ is equal to the Enting-Guttmann result, 2.638 159(1). The value of γ_1 is very close to but slightly larger than, the theoretical value of Cardy, $\gamma_1=\frac{61}{64}=0.953\,12\ldots$; this small difference is probably due to finite-size effects. Notice that the same results, but with larger statistical errors, have been obtained from the sample based on $b=3$; this is an indication that our results are reliable. Similar results, $\gamma_1=0.945\pm0.005$, where obtained by Barber *et al.* [13] from exact enumeration of SAW's on the square lattice. In their analysis, however, they used the best value of μ that was known at that time, $\mu=2.3686$, which is larger than the

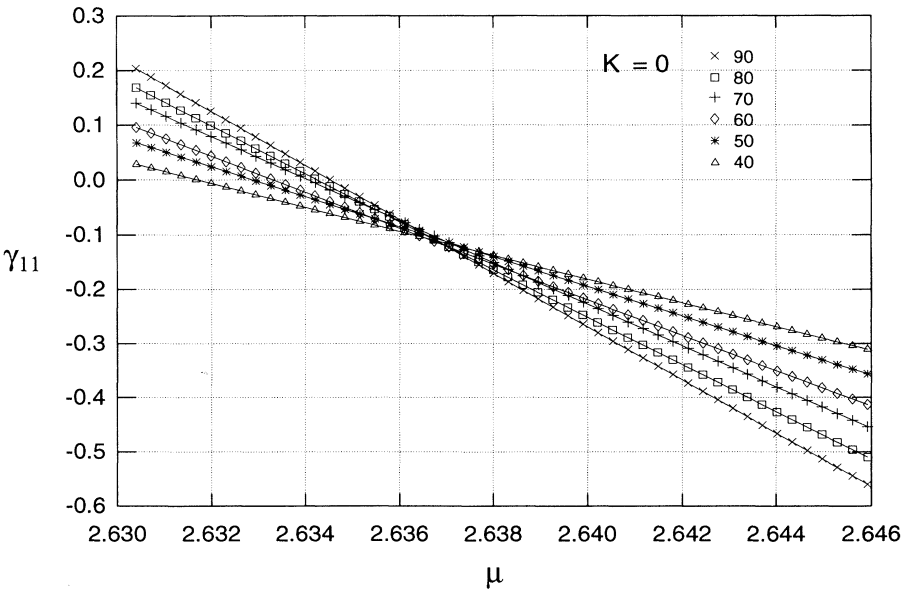

FIG. 6. Plots of $\log_{10}[2Z_{11}(2N)/Z_{11}(N)\mu^N]/\log_{10}2$ vs μ for $N=40,50,\ldots,90$ at $K=0$ (see Fig. 4 caption). The intersection point defines both the correct μ and γ_{11} $(K=0)$.

TABLE IV. Same as Table II for μ and γ_1 at infinite temperature $K=0$, based on figures similar to Fig. 5.

N \ N	120	110	100	90	80	70
			γ_1			
40	0.9553	0.9553	0.9552	0.9552	0.9552	0.9553
50	0.9552	0.9551	0.9551	0.9550	0.9550	
60	0.9552	0.9551	0.9550	0.9549		
70	0.9553	0.9552	0.9550			
			μ			
40	2.638 16	2.638 16	2.638 16	2.638 16	2.638 16	2.638 16
50	2.638 16	2.638 16	2.638 16	2.638 16	2.638 16	
60	2.638 16	2.638 16	2.638 16	2.631 86		
70	2.638 16	2.638 16	2.638 16			

Enting-Guttmann result; therefore, their value of γ_1 (and of γ_{11}, which is discussed later) is slightly too low. De'Bell and Essam [14], using the same technique, obtained for the triangular lattice, $\gamma_1=0.956^{+0.014}_{-0.006}$. Also, very good agreement with the Cardy result has been found by the two transfer-matrix studies [24,25].

The graph for γ_{11} (Fig. 6) does not show a sharp intersection point as that observed in the previous figures; also, it is based only on $N=40-90$. For smaller and larger values of N, the lines were found to deviate from the general trend due to finite-size effects and large statistical errors, respectively. This stems from the fact that the sample contains a relatively small number of chains that also end on the surface (see the results for A_{11} in Table I). Thus, the value of μ at the intersection point, 2.6368(5), is smaller than the correct value; correspondingly, the result, $\gamma_{11}\sim -0.117$, at this point is larger than the expected theoretical value, $\gamma_{11}=-0.1875\ldots$ (obtained from the Barber scaling relations and the Cardy result). Therefore, much larger samples are required in order to obtain the correct results for these quantities. Thus, using the best estimate of μ of Enting and Guttmann, we have calculated four values of γ_{11} for $N=40-80,90$ and $N=50-80,90$. The results are averaged and the statistical error is defined as twice their standard deviation, where the width of the intersection is also taken into account; we obtain

$$\gamma_{11}(K=0)=-0.158\pm0.040\ .$$

This value of γ_{11} is equal, within the error bars, to the Cardy value, -0.187, and leads to

$$2\gamma_1-\gamma_{11}=2.07\pm0.0406\ ,$$

which is equal to $\gamma+\nu=2.09$, i.e., the Barber scaling relation [54,13] is satisfied. Exact-enumeration studies have yielded $\gamma_{11}=-0.19^{+0.03}_{-0.02}$ and $\gamma_{11}=-0.17^{+0.03}_{-0.07}$ in Ref. [13] and [14], respectively.

V. SUMMARY

We have carried out extensive simulations of SAW's anchored to an adsorbing surface on the square lattice. SAW's of up to $N=260$ steps have been studied which are much longer than those treated previously by exact enumeration or computer simulation; samples have been generated with different values of the scanning parameter, $b=3$ and 5. In most cases the different samples lead to the same results, which indicates that they are statistically reliable. Indeed, at the ordinary point our result for

$$\mu=2.638\,16\pm0.000\,02$$

is equal, within the error bars, to the best-known estimate of this quantity in the bulk. Also, our value for γ_1 agrees very well with the Cardy value $\gamma_1=\frac{61}{64}$, obtained from conformal invariance. At the special point we obtain for the first time independent estimates for γ_1 and γ_{11} and, therefore, also two independent estimates for μ. The latter are equal and very close to the Enting-Guttmann value. The result $\gamma_1=1.478\pm0.020$ is slightly larger than the theoretical value of Guim and Burkhardt [24] and than results obtained by other numerical methods; we also find $\gamma_{11}=0.860\pm0.026$. These results for γ_1 and γ_{11} satisfy nicely the Barber scaling relation. However, our transition temperature, $K^*=0.722\pm0.004$, is larger than values obtained by the transfer-matrix method. Correspondingly, our result for the crossover exponent, $\phi=0.562\pm0.020$, is significantly larger than the theoretical value of Burkhardt, Eisenriegler, and Guim [6], $\phi=\frac{1}{2}$, which has been corroborated by transfer-matrix studies. The reason for this discrepancy is unclear, and further studies, numerical and possibly theoretical, will be required.

Note added in proof. After submitting this paper for publication we became aware of a paper by D. Zhao, T. Lookman, and K. D'Bell, Phys. Rev. A **42**, 4591 (1990), in which the present model is studied by exact enumeration. Using the partial-differential approximation method they obtain for the square lattice $K^*=0.72\pm0.05$, $\phi=0.50\pm0.09$, and $\gamma_1=1.45\pm0.05$. For the triangular lattice their results are $\phi=0.51\pm0.01$ and $\gamma=1.4\pm0.1$. These results have relatively large error bars; they agree with the theoretical values and in most cases also with our results.

ACKNOWLEDGMENTS

We thank Y. Shapir and T. W. Burkhardt for helpful discussions. We acknowledge support from the Florida State University Supercomputer Computations Research Institute, which is partially funded by the U.S. Department of Energy under Contract No. DE-FC05-85ER250000. I.C. acknowledges partial support from the Korea Science and Engineering Foundation through Grant No. 923-2000-006-2, from the Science Research Center of Excellence Program, and from the Basic Science Research Institute Program (BSRI-92-234) of The Ministry of Education, Korea.

[1] B. Nienhuis, in *Phase Transition and Critical Phenomena,* edited by C. Domb and J. Lebowitz (Academic, London, 1987), Vol. 11.
[2] J. L. Cardy, in Ref. [1], Vol 11.
[3] B. Duplantier and H. Saleur, Phys. Rev. Lett. **59**, 539 (1987).
[4] C. Vanderzande, A. L. Stella, and F. Seno, Phys. Rev. Lett. **67**, 2757 (1991); A. L. Stella, F. Seno, and C. Vanderzande (unpublished).
[5] J. L. Cardy, Nucl. Phys. B **240**, 514 (1984).
[6] T. W. Burkhardt, E. Eisenriegler, and I. Guim, Nucl. Phys. B **316**, 559 (1989).
[7] T. W. Burkhardt and J. L. Cardy, J. Phys. A **20**, L233 (1987).
[8] P. J. Fory, J. Chem. Phys. **17**, 303 (1949).
[9] P. G. de Gennes, *Scaling Concepts in Polymer Physics* (Cornell University, Ithaca, 1985).
[10] K. Binder, in *Phase Transition and Critical Phenomena,* edited by C. Domb and J. L. Lebowitz (Academic, New York, 1983), Vol. 8.
[11] D. Napper, *Polymeric Stabilization of Colloidal Dispersions* (Academic, New York, 1983).
[12] H. S. Chan and K. Dill, Annu. Rev. Biophys. Biophys. Chem. **20**, 447 (1991).
[13] M. N. Barber, A. J. Guttmann, K. M. Middlemiss, G. M. Torrie, and S. G. Whittington, J. Phys. A **11**, 1833 (1978).
[14] K. De'Bell and J. W. Essam, J. Phys. C **13**, 4811 (1980).
[15] D. C. Rapaport, Phys. Lett. A **48**, 339 (1974).
[16] T. Ishinabe, J. Chem. Phys. **77**, 3171 (1983).
[17] V. Privman, J. Phys. A **19**, 3287 (1986).
[18] F. Seno and A. L. Stella, J. Phys. (Paris) **49**, 739 (1988); Europhys. Lett. **7**, 605 (1989).
[19] D. P. Foster, E. Orlandini, and M. C. Tesi, J. Phys. A **25**, L1211 (1992).
[20] D. J. Klein, J. Stat. Phys. **23**, 561 (1980).
[21] I. G. Enting, J. Phys. A **13**, 3713 (1980).
[22] B. Derrida, J. Phys. A **14**, L5 (1981).
[23] H. Saleur, J. Stat. Phys. **45**, 419 (1991).
[24] I. Guim and T. W. Burkhardt, J. Phys. A **22**, 1131 (1989).
[25] A. R. Veal, J. M. Yeomans, and G. Jug, J. Phys. A **24**, 827 (1991).
[26] N. Metropolis, A. W. Rosenbluth, M. N. Rosenbluth, A. H. Teller, and E. Teller, J. Chem. Phys. **21**, 1087 (1953).
[27] M. N. Rosenbluth and A. W. Rosenbluth, J. Chem. Phys. **23**, 356 (1955).
[28] E. A. DiMarzio and F. L. McCrackin, J. Chem. Phys. **43**, 539 (1965).
[29] P. H. Verdier and W. H. Stockmayer, J. Chem. Phys. **36**, 227 (1962).
[30] Z. Alexandrowicz, J. Chem. Phys. **51**, 561 (1969).
[31] M. Lal, Mol. Phys. **17**, 57 (1969).
[32] F. T. Wall and F. Mandel, J. Chem. Phys. **63**, 4592 (1975).
[33] E. Eisenriegler, K. Kremer, and K. Binder, J. Chem. Phys. **77**, 6296 (1982).
[34] S. Livne and H. Meirovitch, J. Chem. Phys. **88**, 4498 (1988); H. Meirovitch and S. Livne, *ibid.* **88**, 4507 (1988).
[35] P. H. Poole, A. Coniglio, N. Jan, and H. E. Stanley, Phys. Rev. B **39**, 495 (1988).
[36] A. Berretti and A. D. Sokal, J. Stat. Phys. **40**, 483 (1985).
[37] I. S. Chang, H. Meirovitch, and Y. Shapir, Phys. Rev. A **41**, 1808 (1990).
[38] T. M. Birshtein and V. Buldyrev, Polym. Sci. USSR Engl. Transl. **31**, 114 (1989).
[39] H. Meirovitch and H. A. Lim, J. Chem. Phys. **91**, 2544 (1989).
[40] H. Meirovitch, J. Chem. Phys. **89**, 2514 (1988).
[41] I. Chang and H. Meirovitch, Phys. Rev. Lett. **69**, 2232 (1992).
[42] A. Baumgärtner, in *The Monte Carlo Method in Condensed Matter Physics,* edited by K. Binder (Springer, Berlin, 1992).
[43] N. Madras and A. D. Sokal, J. Stat. Phys. **47**, 573 (1987).
[44] K. De'Bell, J. Phys. C **12**, L605 (1979).
[45] K. Kremer, J. Phys. A **16**, 4333 (1983).
[46] R. J. Rubin, J. Chem. Phys. **43**, 2392 (1965).
[47] H. Kahn, in *Symposium on Monte Carlo Methods,* edited by H. A. Meyer (Wiley, New York, 1956), p. 146.
[48] J. M. Hammersley and D. C. Handscomb, *The Monte Carlo Method* (Mathuen, London, 1964).
[49] K. E. Schmidt, Phys. Rev. Lett. **51**, 2175 (1983).
[50] M. N. Barber and W. Selke, J. Phys. A **15**, L617 (1982).
[51] E. Bouchaud and J. Vannimenus, J. Phys. (Paris) **50**, 2931 (1989).
[52] I. Guim and T. W. Burkhardt (unpublished).
[53] I. G. Enting and A. J. Guttmann, J. Phys. A **18**, 1007 (1985).
[54] M. N. Barber, Phys. Rev. B **8**, 407 (1973).